Predicting the Young's Modulus and Uniaxial Compressive Strength of a typical limestone using the Principal Component Regression and Particle Swarm Optimization

Maryam Mokhtari[1*]

1. Department of Civil engineering, Yazd University, Yazd, Iran

Received: 2021/6/6 Accepted: 2021/10/14

Abstract

The rock uniaxial compressive strength (UCS) and modulus of elasticity (E_s) are two key design parameters in geotechnical engineering and rock mechanics. This study tries to accurately predict the desirable parameters using physical characteristics and ultrasonic tests. To do so, two methods, i.e. principal components regression and support vector regression, were employed. The parameters used in modelling included density, P- wave velocity, dynamic Poisson's ratio and porosity. Accordingly, the experimental results conducted on 115 limestone rock samples, including uniaxial compressive and ultrasonic tests, were used and the desired parameters in the modelling were extracted using the laboratory results. By means of coefficient of determination (R^2), normalized mean square error (NMSE) and Mean absolute error (MAE), the developed models were validated and their accuracy were evaluated. The obtained results showed that both methods could estimate the target parameters with high accuracy. In UCS modeling, the values of R^2, NMSE, and MAE obtained from the PCR method for the training set were 0.78, 22.45, and 0.363, respectively. Also, the values of R^2, MSE, and MAE obtained for the testing set were 0.76, 22.51, and 0.357, respectively. In E_s modeling, the values of R^2, MSE, and MAE obtained from the PCR method for the training set were 0.71, 34.23, and 0.421, respectively. Also, the values of R^2, NMSE, and MAE obtained for the testing set were 0.7, 34.23, and 0.43, respectively. In support vector regression, Particle Swarm Optimization method was used for determining optimal values of box constraint mode and epsilon mode, and the modelling was conducted

*Corresponding Author: mokhtari@yazd.ac.ir

using four kernel functions, including linear, quadratic, cubic and Gaussian. Here, the quadratic kernel function yielded the best result for UCS and cubic kernel function yielded the best result for E_s. The values of R^2, NMSE, and MAE were 0.83, 16.98, and 0.329, respectively, for the training dataset using the quadratic function in modeling UCS with the SVR method. Also, the values of MSE, R^2, and MAE obtained for the testing set were 0.76, 22.15, and 0.296, respectively. In E_s modeling, the values of R^2, MSE, and MAE were 0.73, 29.11, and 0.45 for the training set, respectively. Also, the values obtained for R^2, MSE, and MAE were 0.7, 25.67, and 0.272, for the testing set, respectively. In addition, comparing the results of the principal components regression and the support vector regression indicated that the latter outperformed the former.

Keywords: Uniaxial compressive strength, Dynamic young's module, Support vector regression, Principal components regression, Ultrasonic test

1.Introduction

Uniaxial compressive strength (UCS) and static Young's modulus (E_s) are two important aspects of the behaviors observed in intact rocks, playing a crucial role in classification systems of rock bodies and their failure, design stages of engineering projects, and determination of failure behaviors found during drilling operations, tunnel construction, foundation design and dam construction[1-4]. Generally, the commonly used methods to achieve the aforementioned parameters are divided into two groups, namely direct methods based on the measurement (tests) of laboratory specimens and indirect methods based on the estimation of values through desirable empirical equations [2, 5]. The procedure of conducting laboratory tests, commonly used to determine the E_s and UCS of rocks, is standardized by the American Society for Testing and Materials (ASTM) and the International Society for Rock Mechanics (ISRM). In the laboratory, high-quality core specimens are required to directly determine the UCS and E_s. On the other hand, high-quality cores cannot always be extracted from weak, highly fractured, weathered, and thinly bedded rock samples [6, 7]. Furthermore, the exact implementation of the given tests is time-consuming, tedious and costly, requiring a large number of desirable specimens [3, 8]. To overcome these problems, many studies have been conducted to find a fast and efficient way to predict UCS and E_s parameters based on

indirect and non-destructive methods[5]. Compared with the static methods, the ultrasonic approach, as a non-destructive method, makes it possible to achieve the values of some dynamic parameters at little expense without any changes in the internal structure of specimens. Quantities such as density (ρ), P-wave velocity (V_p) and shear wave velocity (V_s), due to two significant advantages of relative cheapness and availability, are among parameters serving to estimate the UCS and E_s. Despite the fact that the acceptability, reliability, and practicality of the static parameters are more than the dynamic parameters, the static parameter measurement is much harder than that of the dynamic ones. This is because the static measurements are strongly influenced by crack, pore pressure and stress-strain. Therefore, finding the correct correlation between the static and dynamic parameters, using indirect methods, is required [1].

In order to achieve empirical relations and equations that yield UCS and E_s values, researchers have lately employed simple regression techniques and multiple regression analyses (MRA)[9-11]. In recent years, probabilistic and soft-computing methods, including artificial neural networks (ANN) [9, 11-20], Bayesian methods [21-23],neural networks and fuzzy systems [7], fuzzy inference systems [10, 16, 24-27], adaptive neuro-fuzzy inference systems [11, 24, 28, 29], support vector regression [12], regression trees[30, 31], genetic programming [2, 32, 33], neural network and genetic algorithm[6, 34], hybrid artificial neural network and particle swarm optimization technique [35, 36], and hybrid neural network and imperialist competitive algorithm [27] have been adopted by researchers in order to estimate the UCS and E_s values.

The aim of the present study is to develop robust and practical models for estimating the UCS and E_s of limestone. Review of the related literature showed that there were few studies focusing on the application of Principal Component Regression **(**PCR) and Support Vector Regression **(**SVR) models so as to predict rock properties. SVR method was only used in a similar study and PCR method was not used for estimation of UCS and E_s. In this study, the UCS and E_s of PCR and SVR models were trained and tested using 115 datasets extracted from the Roud Bar Lorestan Pumped Storage Power Plant project. Index tests, including density (ρ), porosity (*n*), ultrasonic P-wave velocity (V_p), and Poisson's ratio (ν), were used to estimate the UCS and E_s

2.The regression analyses techniques

2.1. Principal Component Regression (PCR)

Principal Component Regression (PCR) is a regression analysis technique, based on principal component analysis (PCA). PCA is used to estimate the unknown regression coefficients in the model. PCR, however, considers regressing the outcome (also known as the dependent variable or the response) on a set of covariates (also known as independent variables, predictors or explanatory variables) based on a standard linear regression model [37, 38]. In PCR, instead of directly regressing the dependent variable on the explanatory variables, the principal components of the explanatory variables are used as regression is done. Only one subset of all principal components is typically used for regression. The principal components with higher variances, that is to say, the ones based on eigenvectors corresponding to the higher eigenvalues of the sample variance-covariance matrix of the explanatory variables, are often selected as regresses. However, to predict the outcome, the principal components having low variances are also significant; in a number of cases, they are even more important[37]. One major use of PCR lies in overcoming the multicollinearity problem arising when two or more explanatory variables are close to collinearity. PCR can aptly deal with such cases by excluding some of the low-variance principal components in the regression step. In addition, typically, by regressing on only one subset of all principal components, PCR can result in the sufficient dimension reduction through substantially lowering the effective number of parameters characterizing the underlying model. This can particularly be useful in settings where high-dimensional covariates exist. Also, through appropriate selection of the principal components to be used for regression, PCR can lead to the efficient prediction of the outcome based on the assumed model [38, 39].

The regression equation in the matrix form is written as follows:

$$Y = XB + e \tag{1}$$

Let $Y_{n\times 1} = (y_1 ... y_n)^T$ denote the vector of observed outcomes and $X_{n\times p} = (x_1 ... x_n)^T$ signify the corresponding data matrix of observed covariates where, n and p indicate the size of the observed sample and the number of covariates respectively, with $n \geq p$. Each of the n rows of X denotes one set of observations for the p dimensional covariate and the respective entry of Y represents the corresponding observed outcome. Assume that Y and

each of the p columns of X have already been centered so that all of them have zero empirical means. This centering step is crucial (at least for the columns of X) since PCR involves the use of PCA in X . PCA is also sensitive to the data centering [39].

$B \in R^p$ denotes the unknown parameter vector of regression coefficients and e represents the vector of random errors.

The primary goal is to obtain an efficient estimator $\hat{B}$ for the parameter B , based on the available data. One frequently used approach for this purpose is ordinary least squares regression in which, assuming X is the full column rank, the unbiased estimator $\hat{B}_{ols} = (X^T X)^{-1} X^T Y$ of B is achieved. PCR is another technique used for the same purpose of estimating B [39].

2.2. Support Vector Regression (SVR)

Data classification is a common task in machine learning. Support Vector Machines (SVM) are learning machines that to obtain good generalization on a limited number of learning patterns used the structural risk minimization inductive principle, first identified by Vladimir Vapnik and his colleagues in 1992 [40]. Suppose some given data points, each belonging to one of the two classes, where the goal is to decide in which class a new data point will place. In the case of support vector machines, a data point is viewed as a p-dimensional vector (a list of p numbers). Here, the goal is to find whether or not such points can be separated with a $(p-1)$-dimensional hyperplane. This is called a linear classifier. There are many hyperplanes that can classify the data. Concerning the best hyperplane, one reasonable choice is the one representing the largest separation, or margin, between the two classes. Thus, the authors select the hyperplane whose distance from the nearest data point on each side is maximized. If such a hyperplane exists, it is known as a maximum-margin hyperplane; the linear classifier it defines is known as a maximum-margin classifier; or equivalently, the perceptron of the optimal stability [41, 42]. SVM implements a learning algorithm, useful for recognizing subtle patterns in complex data sets. The algorithm performs discriminative classification learning, for example, to predict the classifications of previously unseen data. There are two main categories for support vector machines, i.e. support vector classification (SVC) and support vector regression (SVR). The model developed by SVR only depends on a subset

of the training data because the cost function for building the model ignores any training data that is close to the model prediction [43].

Suppose we have a set of training data where x_n is a multivariate set of *N* observations with observed response values y_n [40]. To find the below linear function:

$$f(x) = x'\beta + b \tag{2}$$

and ensure that it is as flat as possible, *f*(*x*) with minimal norm values ($\beta\beta'$) is found. This is formulated as a convex optimization problem to minimize the following equation:

$$J(\beta) = \frac{1}{2}\beta'\beta \tag{3}$$

which is subject to all residuals having a value less than ε, or, in an equation form:

$$\forall_n : \left| y_n - (x_n'\beta + b) \right| \le \varepsilon \tag{4}$$

There are a number of cases in which no such function f(x) exists to satisfy the mentioned constraints for all points. To deal with the possible infeasible constraints, slack variables ξ_n and ξ_n^* are introduced for each point. This approach is similar to the "soft margin" concept in SVM classification because the slack variables allow regression errors to exist up to the value of ξ_n and ξ_n^*, while satisfying the required conditions. Including slack variables leads to the objective function, also known as the primal formula[39, 44]:

$$J(\beta) = \frac{1}{2}\beta'\beta + C\sum_{n=1}^{N}(\xi_n + \xi_n^*) \tag{5}$$

Which is subject to:

$$\forall_n : y_n - (x_n'\beta + b) \le \varepsilon + \xi_n \tag{6}$$

$$\forall_n : (x_n'\beta + b) - y_n \le \varepsilon + \xi_n^* \tag{7}$$

$$\xi_n^* \ge 0 \tag{8}$$

$$\xi_n \ge 0 \tag{9}$$

The constant *C* is the box constraint, a positive numeric value that controls the penalty imposed on observations lying outside the epsilon margin (ε) and helps to prevent overfitting (regularization). This value determines the trade-off between the flatness of *f(x)* and the amount up to which deviations larger than ε are tolerated. The linear ε-insensitive loss function ignores errors that are within ε distance of the observed value by treating them as equal to zero. The loss is measured based on the distance between the observed value y and the ε boundary. This is formally described by the following equation:

$$\begin{cases} 0 & |y-f(x)| \le \varepsilon \\ |y-f(x)|-\varepsilon & otherwise \end{cases} \quad (10)$$

The optimization problem previously described is computationally simpler to solve in its Lagrange dual formulation. The solution to the dual problem provides a lower bound to the solution of the primal (minimization) problem. The optimal values of the primal and dual problems need not be equal, and the difference is called the "duality gap." However, when the problem is convex and satisfies a constraint qualification condition, the value of the optimal solution to the primal problem is given by the solution of the dual problem.

To obtain the dual formula, a Lagrangian functionshould be constructed from the primal function by introducing nonnegative multipliers α_n and α_n^* (Lagrange multiplier) for each observation x_n. This leads to the dual formula, where the following equation is minimized[43]:

$$L(a)=\frac{1}{2}\sum^{N}\sum^{N}(a_i-a_i^{\circ})(a_i-a_i^{\circ})x_i^{'}+\varepsilon\sum^{N}(a_i-a_i^{\circ})+\sum^{N}y_i(a_i^{\circ}-a) \quad (11)$$

which is subject to the following constraints:

$$\sum_{n=1}^{N}(\alpha_n-\alpha_n^*)=0 \quad (12)$$

$$\forall_n : 0 \le \alpha^*{}_n \le C \quad (13)$$

$$\forall_n : 0 \le \alpha_n \le C \quad (14)$$

where the β parameter can completely be described as a linear combination of training observations using the equation below:

$$\beta=\sum_{n=1}^{N}(\alpha_n-\alpha_n^*)x_n \quad (15)$$

The function *f(x)* is then equal to[43]:

$$f(x)=\sum_{n=1}^{N}(\alpha_n-\alpha_n^*)(x_n^{'}x)+b \quad (16)$$

For linear SVR, the conditions are as follows:

$$\forall_n : a_n(\varepsilon+\xi_n-y_n-x_n^{'}\beta+b)=0 \quad (17)$$

$$\forall_n : a_n^*(\varepsilon+\xi_n^*+y_n-x_n^{'}\beta-b)=0 \quad (18)$$

$$\forall_n : \xi_n(C-\alpha_n)=0 \quad (19)$$

$$\forall_n : \xi_n^*(C-\alpha_n^*)=0 \quad (20)$$

Some regression problems cannot adequately be described using a linear model. In such a case, the Lagrange dual formulation allows the previously described technique to be extended to nonlinear functions.

Accordingly, a nonlinear SVR model is obtained by replacing the dot product $x_1^{'}x_2$ with a nonlinear kernel function $G(x_1, x_2) \leq \varphi(x_1), \varphi(x_2) >$, where $\varphi(x)$ is a transformation that maps x to a high-dimensional space. Statistics and Machine Learning Toolbox provide the following built-in semi-definite kernel functions.

The Gram matrix is an *n*-by-*n* matrix containing elements $g_{ij} = G(x_i, x_j)$. Each element g_{ij} is equal to the inner product of the predictors as transformed by φ. However, there is no need to know φ because the kernel function can be used to directly generate the Gram matrix. Using this method, the nonlinear SVR finds the optimal function *f(x)* in the transformed predictor space.

The dual formula for nonlinear SVR replaces the inner product of the predictors (x_i, x_j) with the corresponding element of the Gram matrix (g_{ij}). Nonlinear SVR finds the coefficients that minimize the equation below:

$$L(a) = \frac{1}{2}\sum_{i=1}^{N}\sum_{j=1}^{N}\left(a_i - a_i^{\circ}\right)\left(a_j - a_j^{\circ}\right)G\left(x_i, x_j\right) + \varepsilon\sum_{i=1}^{N}\left(a_i + a_i^{\circ}\right) - \sum_{i=1}^{N} y_i\left(a_i - a_i^{\circ}\right) \quad (21)$$

These conditions indicate that all observations, strictly inside the epsilon tube, have Lagrange multipliers $\alpha_n = 0 \; and \; \alpha_n^* = 0$. Observations with nonzero Lagrange multipliers are called support vectors. The functions used to predict new values only depends on the support [39-42]:

$$f(x) = \sum_{n=2}^{N}\left(a_n - a_n^{\circ}\right)G(x_n, x) + b \quad (22)$$

Several kernel functions are available in the literature [45]. In this study, the authors employed four kernel functions, i.e. linear, quadratic, cubic and gaussian functions, in the prediction model concerning UCS and E_s.

2.3.Performance Evaluation

The performance of the developed models was evaluated by means of three criteria, including coefficient of determination (R^2), normalized mean square error (NMSE), and mean absolute error (MAE). These criteria were defined as follows:

$$R^2 = \frac{\left[\sum_{i=1}^{N}(P_i - \overline{P})(M_i - \overline{M})\right]^2}{\left[\sum_{i=1}^{N}(P_i - \overline{P})^2(M_i - \overline{M})^2\right]} \quad (23)$$

$$NMSE = \frac{\sum_{i=1}^{N}(M_i - P_i)^2}{\sum_{i=1}^{N}(M_i)^2} \times 100 \quad (24)$$

$$MAE = \frac{1}{(24)}\sum_{i=1}^{N}|M_i - P_i| \quad (25)$$

In the above relationships, N is the number of samples, P_i and M_i are the predicted and measured output values, and $\overline{P}$ and $\overline{M}$ are the means of the predicted and measured outputvalues.

3.Rock characteristics and testing procedures

The samples examined in this study were the cylindrical core samples of limestone collected from 10 exploratory boreholes located near the powerhouse cavern of the Roud Bar Lorestan pumped storage power plant project (RL-PSPP), Lorestan province, Iran (Fig.1). The powerhouse is located in the thick light- to dark-gray limestone and dolomite limestone layer of Dalan formation (Fig. 2). The bedding dip of this formation is mostly semi-vertical (about 70 – 80 degrees toward west). The Area of this study is located in folded - thrust zone of Zagros. It has been under the effect of several stresses. This has resulted in the creation of faults, folding and joints in the rock. The objective of (RL-PSPP) is to make use of the potential hydropower energy by utilizing pumping system of the national electricity network under low-load conditions and generating energy by means of the turbine and generator to meet the demands of peak loads in the country.

The geotechnical studies mostly aimed to review the underground geology and determine the geotechnical parameters for designing the powerhouse. Table (1) presents specifications of exploratory boreholes. Figure 3 also depict their locations. According to the log of BH29 Borehole exactly drilled at the shaft location, the bedding was an alternation of limestone to dolomitic limestone (Dalan-dolomitic limestone) derived from the beginning to the elevation of about 2100 m and limestone (Dalan-limestone) obtained from the elevation ranging from 2100 to about 1650 m (end of the borehole). The samples were taken from the borehole drilled at (RL-PSPP) Site, presented in Table (1).

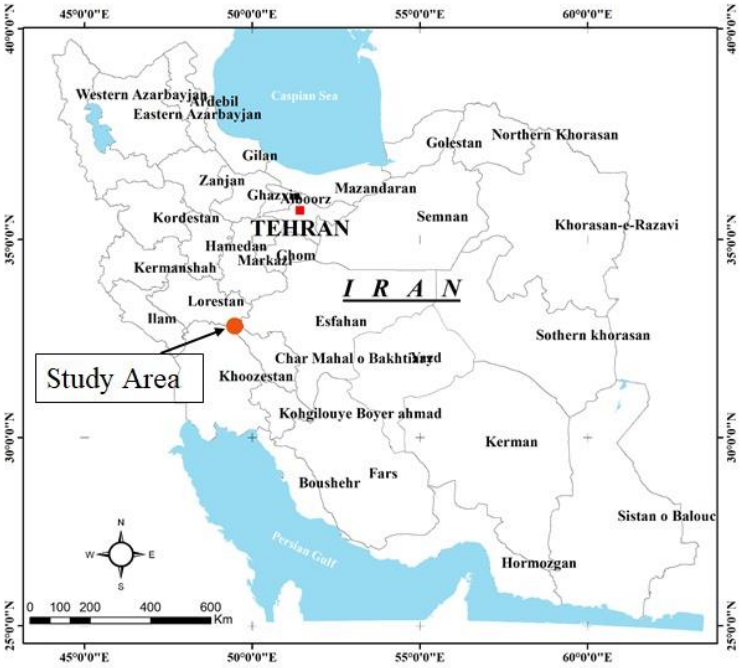

Fig 1. Map showing location of RLPS

Fig 2. Dalan Limestone

Table 1. Specifications of Drilled Exploratory Boreholes

Borehole	Depth (m)	Number of rock samples
BH-232	60	39
BH-233	60	31
BH-234	50	15
BH-235	100	20
HF-1	100	30
HF-2	46.6	5
D-1	61.5	20
D-2	50	17
D-3	50	18
BH-29	384	103

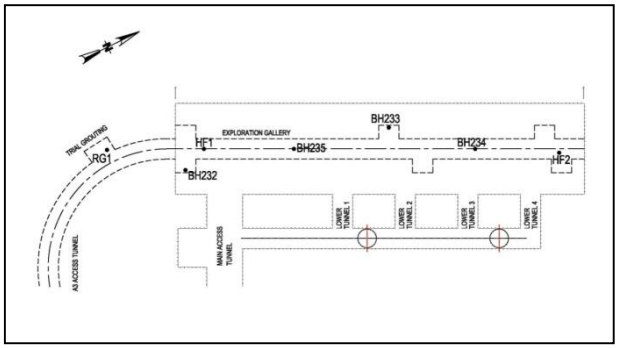

Fig. 3. Boreholes Location around Exploratory Gallery of Powerhouse Cavern Ceiling

As it was mentioned, laboratory experiments were carried out to determine the geomechanical parameters of intact rock and rock masses around the underground structures (powerhouse and transformer caverns) of Roud Bar Lorestan Pumped Storage Power Plant project.

The preparation of the specimens was conducted according to the proposed ISRM approach (2009)[46]. The ends of the specimens were cut and flattened to be accurately perpendicular to the sample's axis. The specimens were smoothed and polished based on the ISRM suggested methods, and also were inspected to be free of macroscopic structures like cracks and other planes of weakness. In order to prevent any noise impact in measurements, the preparation of samples was cautiously followed. The tests were carried out in the laboratory under saturation condition.115 high-quality specimens were eventually prepared with 54 mm to 82 mm diameters and the length-to-diameter proportions of between 2 and 3.

It is necessary to mention, Iran Water and Power Resources Development Company was the owner of the RL-PSPP and Mahab Ghodss Consulting engineering company was the project consultant and conducted the laboratory tests.

These specimens were subjected to a non-destructive ultrasonic test, and their P-wave velocity was measured using a pundit tool. The estimates time and the transmitter-receiver distance were used to calculate the P and S waves' velocities. The real time interval across the sample together with the time delay because of the electronic components, transducer and bonds gives the travel time. Hence, separate measurement of the time delay for P and S waves was first performed prior to measuring the travel time, using a standard such as aluminum samples with specified velocities or face-to-face methods [4٦]. the design of the transmitter aimed at generating wavelengths three times the rock's mean grain size to decrease the first arrivals at the receiver which were scattered and inadequately characterized. Wavelength indicates the division of the wave velocity within the rock sample by the transducer resonant frequency. Frequencies between 75 kHz and 3 MHz are more common to use. Evaluations were made using the PUNDIT together with two transducers, a transmitter, as well as a receiver with 1 MHz frequency. The ultrasonic device is represented in Figure 4. Application of a constant stress around 10 N/cm2 in the axial direction to the samples [46] aimed at improving the ratio of signal/noise. In addition, surface contact of the transducers and samples was improved using an ultrasonic couplant, significantly improving the ratio of signal/noise [46].

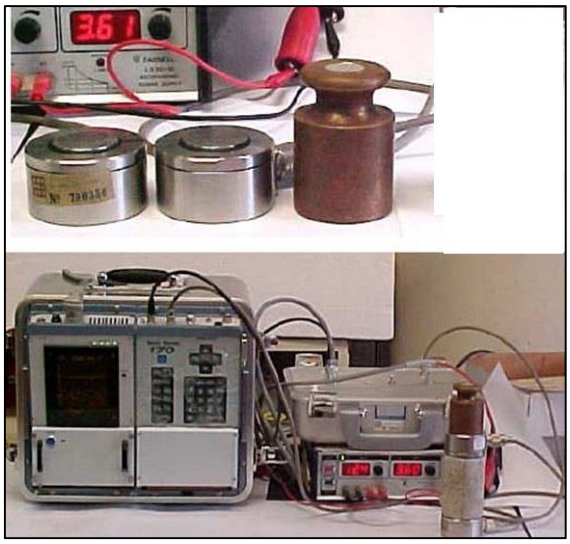

Fig. 4. Apparatuses of ultrasonic testing for determination of primary wave velocity (Vp), and shear wave velocity (Vs)

Following ultrasonic tests, the samples were tested by a uniaxial compressive strength test to measure their static Young's modulus and Poisson's coefficients (Fig. 5). Also, the porosity and density of the specimens were experimentally determined. The fundamental statistics and probability plot of the results obtained from these experiments are given in Table 2 and Figure 6.

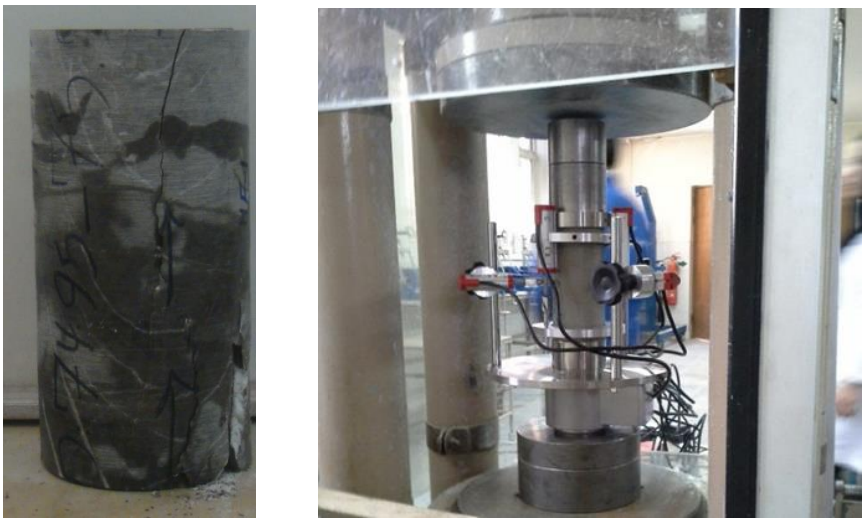

Fig.5. Examples of failure modes observed in limestone loaded in the Uniaxial Compression Test (Core specimens are ~82 mm in diameter)

Table 2. Basic statistics of the results obtained from the tests

Parameters	Unit	Symbol	Minimum	Maximum	Mean	Std.dev.	VIF
Uniaxial compressive strength	MPa	UCS	23.06	188.85	93.83	34.12	-
Static Young' modulus	GPa	E_s	6.19	69.60	27.93	10.51	-
P-wave velocity	m/s	V_P	2088.8	6901.4	5504.87	898.48	1.508
Density	kg/m^3	ρ	2.60	2.78	2.70	0.028	1.104
Poisson's ratio	-	υ	0.18	0.30	0.23	0.0274	1.364
Porosity	%	n	0.17	4.98	1.14	1.09	1.288

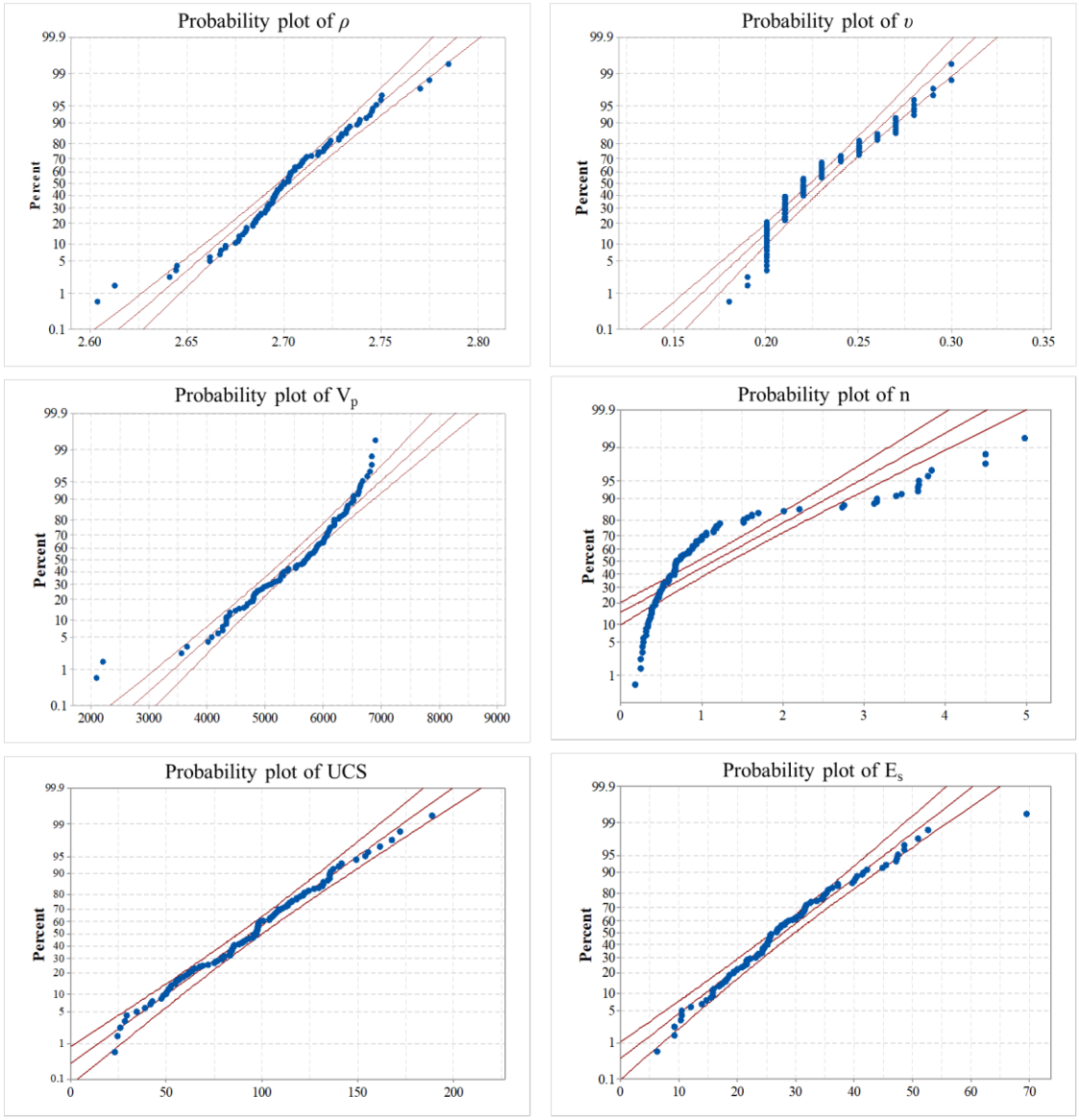

Fig. 6. Probably plots of the results obtained from the tests

4.Model implementation and results

As it is clearly demonstrated in Table 2 and figure 6, these parameters have non-normal distributions; therefore, these distributions should be transformed were normalized for PCR and SVR. The correlation between rock parameters and output data were calculated (Table 3). The results demonstrated that correlations between input and output parameters are statistically significant through hypothesis testing.

Table 3. Correlation between rock parameters and output data (values in bold are different from 0 with a significance level alpha=0.05)

	ρ	υ	Vp	n
UCS	0.194	-0.884	0.363	-0.307
Es	0.238	-0.832	0.324	-0.252

Combinations of V_p, ρ, υ, n, were employed to estimate the UCS and E_s of the limestone rocks by PCR and SVR models. To develop and test the models, 80% of data was randomly selected and assigned to the learning subset to be used for network training; the rest 20% was assigned to the testing subset to be reserved for performance evaluation. Different researchers have used different proportions of data for testing and training in their studies. For the test dataset it can varies between 20 and 25% of data and the remaining for training [48, 49, 50]. The performance of the PCR and SVR models was evaluated by (R^2), (NMSE), and (MAE). The result of PCR models for predicting UCS and E_s are shown in Table 4. To confirm the confidence of obtained results of PCR, Analysis of variance is used (table 5, 6). F-test results showed that the PCR model is valid.

Table 4. Summary of the PCR for predicting UCS and E_s

Model		Train			Test		
		R^2	NMSE	MAE	R^2	NMSE	MAE
PCR	UCS	0.78	22.45	0.363	0.76	22.51	0.357
	E_s	0.71	34.23	0.421	0.70	34.24	0.440

Table 5. Analysis of variance for the result of PCR model for predicting UCS

Source	DF	Sum of squares	Mean squares	F	Pr> F
Model	4	79.160	19.790	81.259	< 0.0001
Error	90	21.919	0.244		
Corrected Total	94	101.079			

Computed against model Y=Mean(Y)

Table 6. Analysis of variance for the result of PCR model for predicting E_s

Source	DF	Sum of squares	Mean squares	F	Pr> F
Model	4	66.104	16.526	53.266	< 0.0001
Error	90	27.923	0.310		
Corrected Total	94	94.027			

Computed against model Y=Mean(Y)

The optimal values of SVR model parameters were determined by using Particle Swarm Optimization (PSO) method [51, 52]. PSO provide the excellent performance and effective in finding the most optimal solutions. The PSO is a bioinspired stochastic

optimization technique developed simulating social behavior of animals, as was the mass movement of birds. In fact, the PSO algorithm consists of a certain number of particles that randomly take the initial value. A particles considered as a bird in a swarm consisting of a number of birds, and all particles fly through the searching space by following the current optimum particle to find the final optimum solution of the optimization problem. Optimal values of C (box constraint mode) and ε (epsilon mode) were determined by PSO for individual kernel functions. The best performance of PSO-SVR model for predicting UCS and ES for training and testing data with respect to individual kernel functions are shown in Table 7.

Table 7. Summary of the PSO-SVR for predicting UCS and E_s

Model	Kernel function		ε	C	Train			Test		
					R^2	NMSE	MAE	R^2	NMSE	MAE
SVR	Linear	UCS	0.279	1	0.78	22.56	0.342	0.77	18.83	0.278
		E_s	0.593	100	0.70	34.33	0.470	0.66	29.31	0.460
	Quadratic	UCS	0.356	1	0.83	16.98	0.329	0.76	22.15	0.296
		Es	0.85	1	0.73	29.11	0.450	0.70	25.67	0.372
	Cubic	UCS	1.108	1	0.66	43.30	0.572	0.75	23.74	0.272
		Es	0.517	1	0.80	20.12	0.379	0.77	23.37	0.376
	Gaussian	UCS	0.445	1	0.89	13.65	0.187	0.68	38.4	0.330
		Es	0.439	30	0.88	13.63	0.337	0.53	47.95	0.534

According to Tables 4 and 7, the PCR and PSO-SVR models showed reasonable accuracy in estimating the UCS and E_s of limestone. Quadratic-SVR, however, did the best in estimating the UCS and cubic did the best in estimating the E_s. Also, the calculated Statistical indexes for the training and testing subsets were very much close to one another, indicating the appropriacy of the modeling process and the resulting models. In particular, with the help of quadratic kernel functions, PSO-SVR model could perform the best in training and testing the data for the UCS. The training data set showed R^2, NMSE, and MAE values equal to 0.83, 16.98, and 0.329 for prediction of UCS, respectively. Corresponding values for testing data were 0.76, 22.15 and 0.296, respectively. Also, cubic kernel functions to predict E_s: R^2, NMSE, and MAE values revealed 0.80, 20.12 and 0.379 for training data set. Corresponding values for testing data were 0.77, 23.37 and 0.376, respectively. In Table 8 some of the former works in which

different prediction techniques are used have been presented. It can be inferred that our results are comparable with some of results in this table. The results obtained from PCR and PSO-SVR model were plotted against the actual measurement in Figures 7 – 16. All the points, including those pertaining to the trained and tested cases, were almost located within the angle bisector.

Table 8. Comparison some of the former works in which different prediction techniques reported in the literature

References	Technique	Input	Output	R^2
Gokceoglu[23]	FIS	PC	UCS	0.92
Gokceoglu and Zorlu[9]	FIS	Vp, BPI, PLS, TS	UCS, E_s	0.67 for UCS, 0.79 for E
Sonmez et al. [16]	ANN	UCS, UW	E_s	0.67
Karakus and Tutmez[25]	FIS	PLS, SH, Vp	UCS	0.97
Zorlu et al. [18]	ANN	PD, C, Q	UCS	0.67
Yilmaz and Yuksek[10]	ANFIS	SH, PLS, WC, Vp	UCS, E_s	0.94 for UCS, 0.96 for E
Gokceoglu et al. [24]	FIS	CC, SD	UCS	0.88
Canakci et al. [32]	GP	Vp, WA, q	UCS	0.88
Dehghan et al.[11]	ANN	n, SH, PLS, Vp	UCS, E_s	0.86 for UCS, 0.77 for E
Cevik et al. [13]	ANN	SD, CC	UCS	0.97
Yagiz et al. [17]	ANN	UW, SH, n, Vp, SD	UCS, E_s	0.50 for UCS, 0.71 for E
Singh et al. [15]	ANFIS	PLS, q, WA	E_s	0.66
Mishra and Basu[26]	FIS	BPI, PLS, SH, Vp	UCS	0.98
Beiki et al. [31]	GP	q, n, Vp	UCS, E_s	0.83 for UCS, 0.67 for E
Ceryan[12]	SVR	n, PDI	UCS	0.77
Momeni et al.) [33]	PSO–ANN	q, Vp, PLS, SH	UCS	0.97
TonnizamMohamad et al. [34]	PSO–ANN	PLS, TS, q, Vp	UCS	0.97
Ghasemi et al .[2]	M5P	UW, SH, n, Vp, SD	UCS, E_s	0.89 for UCS (unpruned), 0.84 for E_s (unpruned); 0.80 for UCS (pruned), 0.87 for E_s (pruned)
JahedArmaghani et al. [3]	ICA–ANN	SH, PLS, Vp	UCS	0.94
This study	PCR, PSO-SVR	Vp, ρ, υ, n,	UCS, E_s	0.78 for UCS, 0.71 for E_s (PCR). 0.83for UCS (quadratic-SVR), 0.80 for E_s (cubic-SVR)

Equotip hardness (EH),quartz content (q), grain size (GS), rock type (RT),petrographic composition (PC), block punch index (BPI), point load strength (PLS),tensile strength (TS), unit weight (UW), schmidt hardness (SH),packing density (PD), concave–convex (C), water content (WC), clay content (CC), slake durability index (SD), water absorption (WA), P-durability index (PDI), artificial neural network (ANN), fuzzy inference system (FIS), adaptive neuro-fuzzy inference system (ANFIS), genetic programming (GP), imperialist competitive algorithm (ICA)

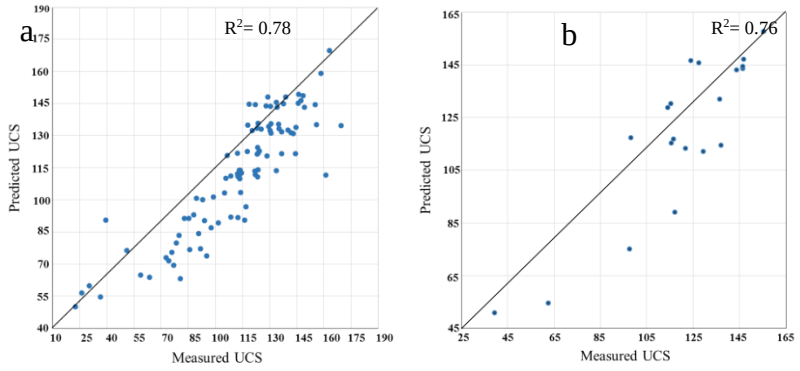

Fig.7. Predicted UCS by the PCR model versus the measured data: (a) Training dataset, (b) Testing dataset

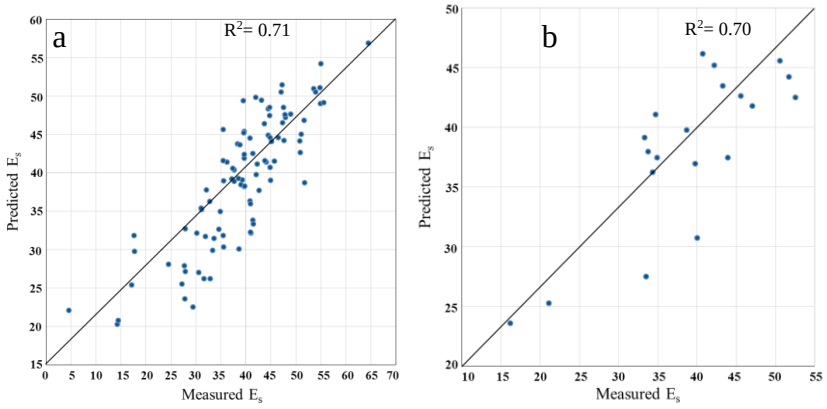

Fig.8. Predicted E_s by the PCR model versus the measured data: (a) Training dataset, (b) Testing dataset

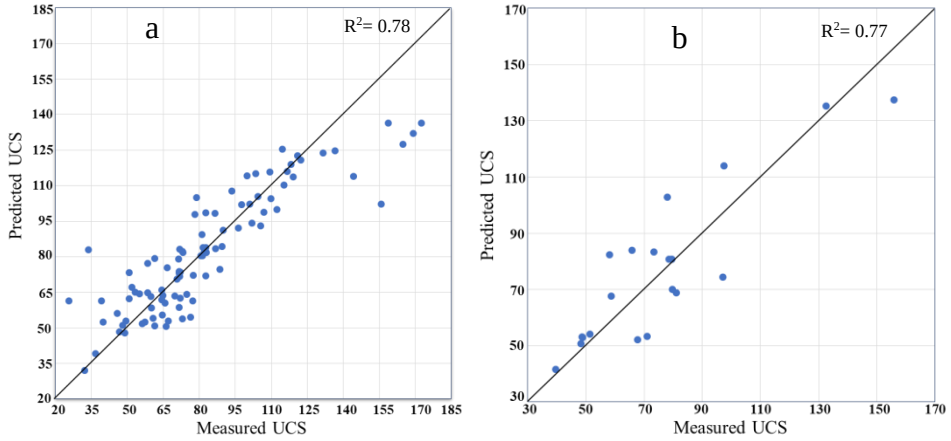

Fig.9. Predicted UCS by the PSO-SVR model versus the measured data (linear function): (a) Training dataset, (b) Testing dataset

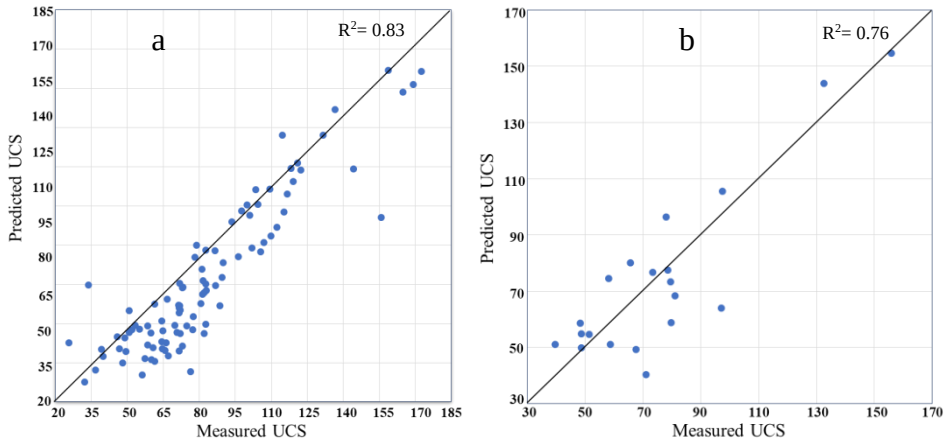

Fig.10. Predicted UCS by the PSO-SVR model versus the measured data (quadratic function): (a) Training dataset, (b) Testing dataset

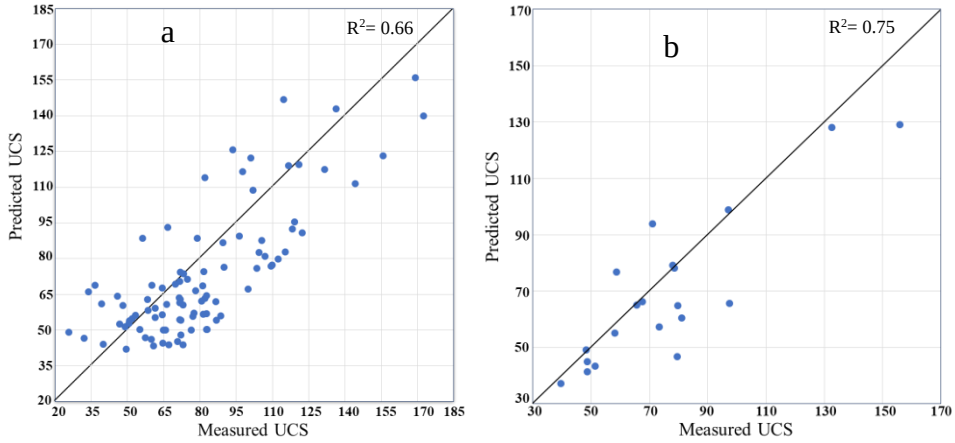

Fig.11. Predicted UCS by the PSO-SVR model versus the measured data (cubic function): (a) Training dataset, (b) Testing dataset

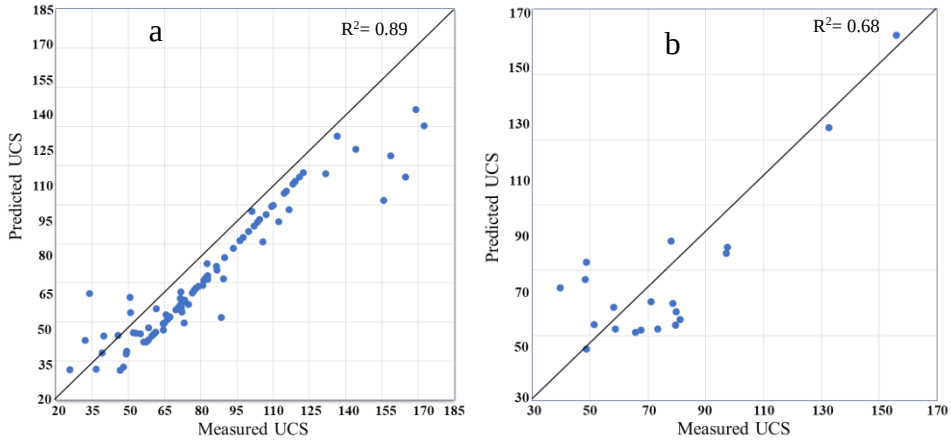

Fig.12. Predicted UCS by the PSO-SVR model versus the measured data (Gaussian function): (a) Training dataset, (b) Testing dataset

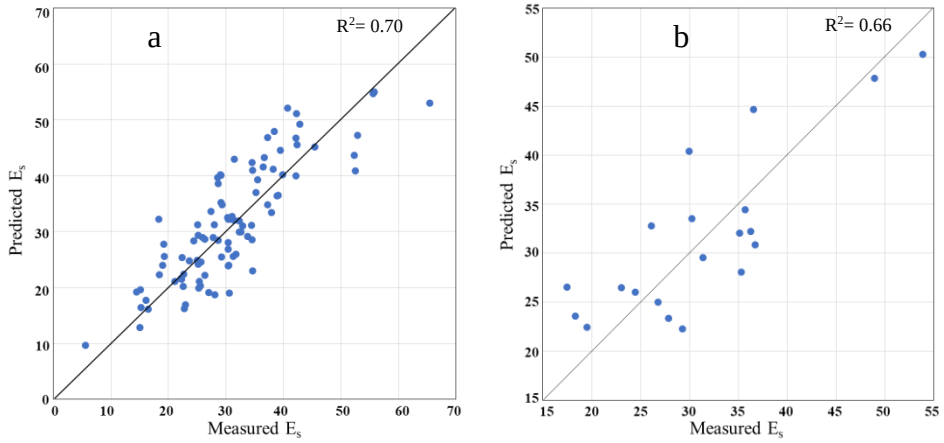

Fig.13. Predicted E_s by the PSO-SVR model versus the measured data (linear function): (a) Training dataset, (b) Testing dataset

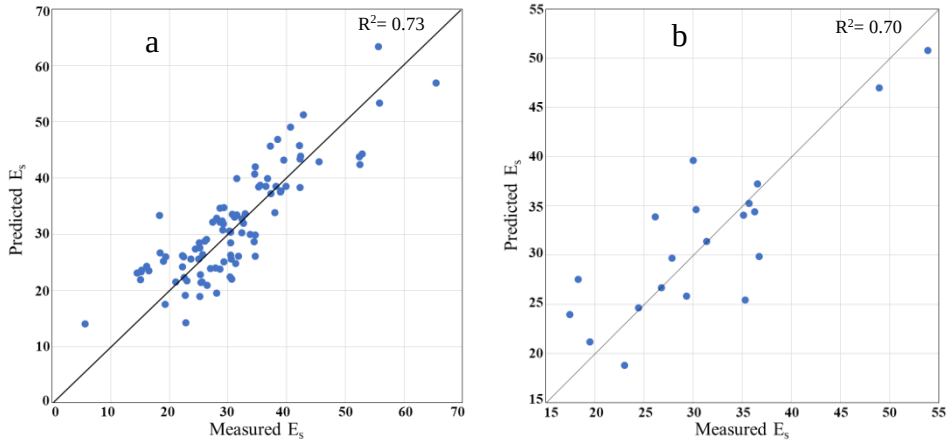

Fig.14. Predicted E_s by the PSO-SVR model versus the measured data (quadratic function): (a) Training dataset, (b) Testing dataset

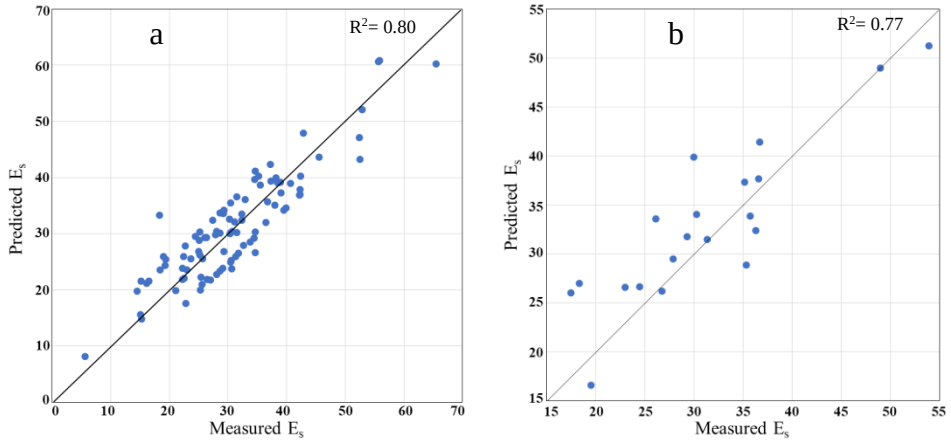

Fig.15. Predicted E_s by the PSO-SVR model versus the measured data (cubic function): (a) Training dataset, (b) Testing dataset

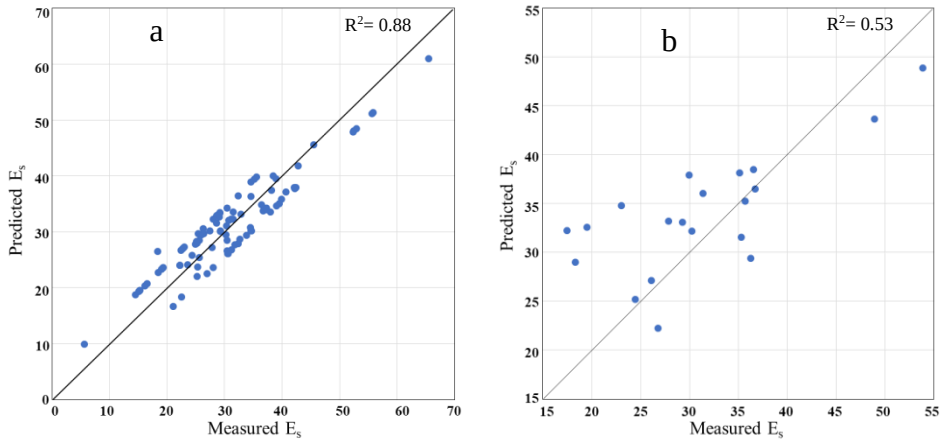

Fig.16. Predicted Es by the PSO-SVR model versus the measured data (Gaussian function): (a) Training dataset, (b) Testing dataset

Figures 7 and 8 show the results of the values predicted in the PCR method for UCS and elastic modulus, respectively. It is clearly obvious that these estimated values by PCR for UCS show less dispersion and fall closer to 45 degree line. However, PCR method is less accurate than UCS in estimating the elastic modulus while greater dispersion is observed. Also, the predicted values for UCS parameters which had been optimized by SVR method and obtained by PSO method are shown in figures 9-11. As Figure 9 shows, the dispersion is high when a linear function is used and a significant difference is observed between the values obtained from the model and the actual values. In addition, Figure 11 indicates that the best prediction belongs to the Gaussian function. Figures 12 to 16 also show the performance of the SVR method in estimating the elastic modulus. In this case, it is observed that the results from the linear function in the SVR method are weaker than the other cases while a considerable dispersion is seen in the results. Fig. 15 shows that the best results are obtained when the SVR method is used along with a Gaussian function. It should also be noted that cubic and quadratic functions fall between the linear function and the Gaussian Function in terms of accuracy.

An examination of Table 8 shows that the neural network and fuzzy systems were traditionally used in estimating the elastic modulus and compressive strength of rocks. One of the methods used in the present study is PCR that has not been used previously. The results of this method are comparable to the methods listed in Table 8. This study also made use of SVR method in combination with the PSO optimization algorithm. Here, the optimization algorithm is used to solve the local minima problem.

5.Conclusions

In this study, two techniques of support vector regression (SVR) and principal component regression (PCR) were used to model the elasticity modulus and uniaxial compressive strength of limestone rocks. Parameters of compressive wave velocity, density, porosity, and Poisson's ratio were used to empirically model the uniaxial strength and elasticity modulus. As mentioned in the introduction, various methods have been used to estimate target parameters using data mining methods. One of the usual methods is regression. One of the problems of regression method is the multicollinearity between input parameters, and also one of the major flaws of statistical relationships is estimating average values, which perhaps can lead to overestimating the low values of UCS and Es, and vice versa. But, the PCR method compared to other regression methods, it has the following advantages: Dimensionality, reduction, Avoidance of multicollinearity between predictors and Overfitting mitigation. Another commonly used technique is the neural network. The major disadvantages of neural networks are the local minima problem and greater computational burden. The SVR method comparison with the neural network does not have the local minima problems, SVR method are considered the nonlinear relationships between parameters, and the error rate is controlled. Comparison of the results of implementing two methods showed that both could estimate the desired parameters with acceptable accuracy. Modeling was performed using four linear, quadratic, cubic and gaussian functions. Based on the obtained results, the SVR method, with the help of quadratic kernel functions, yielded the best result for estimating UCS and cubic kernel function yielded the best result for estimating E_s.

Finally, it can be declared that the target parameters could easily and accurately be estimated by applying the two methods used in this study and these models can be used for other carbonate rocks with similar physical and mechanical parameters.

6.Acknowledgement

The authors acknowledge the Iran water and power resources development company, Mahab Ghodss consulting Engineering Company for approval to use geological and rock mechanics records of the Azad pump storage power plant project.

References

1. Aboutaleb S., Behnia M., Bagherpour R., Bluekian B., "Using non-destructive tests for estimating uniaxial compressive strength and static Young's modulus of carbonate rocks via some modeling techniques", Bulletin of Engineering Geology and the Environment,(2017) 1-12. DOI: 10.1007/s10064-017-1043-2

2. Ghasemi E., Kalhori H., Bagherpour R., Yagiz S., "Model tree approach for predicting uniaxial compressive strength and Young's modulus of carbonate rocks", Bulletin of Engineering Geology and Environment, Vol. 77(1) (2016) 331-334. DOI:10.1007/s10064-016-0931-1

3. Jahed Armaghani D., Tonnizam Mohamad E., Momeni E., Narayanasamy M., MohdAmin M., "An adaptive neuro-fuzzy inference system for predicting unconfined compressive strength and Young's modulus: a study on Main Range granite", Bulletin of Engineering Geology and Environment, Vol. 74(4) (2015) 1301–1319. DOI: 10.1007/s10064-014-0687-4

4. Majdi A., Rezaei M., "Prediction of unconfined compressive strength of rock surrounding a roadway using artificial neural network", Neural Computing and Applications, Vol. 23 (2013) 381–389. DOI:10.1007/s00521-012-0925-2

5. Aladejare A.E., "Evaluation of empirical estimation of uniaxial compressive strength of rock using measurements from index and physical tests", Journal of Rock Mechanic and Geotechnical Engineering, Vol. 12(2) (2020) 256-268.

6. Monjezi M., Khoshalan H. A., Khoshalan M., "A neuro- genetic network for predicting uniaxial compressive strength of rocks", Geotechnical and Geological Engineering, Vol. 30(4) (2012) 1053-1062. DOI: 10.1007/s10706-012-9510-9

7. Sharma L. K., Vishal V., Singh T. N. " Developing novel models using neural networks and fuzzy systems for the prediction of strength of rocks from key geomechanical propertie", Journal of Measurement, Vol. 102 (2017) 158-169. DOI:10.1016/j.measurement.2017.01.043

8. Ghafoori M., Rastegarnia A., Lashkaripour G. R., "Estimation of static parameters based on dynamical and physical roperties in limestone rocks", Journal of African Earth Sciences, Vol. 137 (2018) 22-31. DOI: 10.1016/j.jafrearsci.2017.09.008

9. Gokceoglu C., Zorlu K., "A fuzzy model to predict the uniaxial compressive strength and the modulus of elasticity of a problematic rock", Engineering Applications of Artificial Intelligence, Vol. 17(1) (2004) 61–72. DOI: 10.1016/j.engappai.2003.11.006

10. Yilmaz L., Yuksek G., "Prediction of the strength and elasticity modulus of gypsum using multiple regression, ANN, and ANFIS models", International Journal Rock Mechanic and Mining Science, Vol. 46(4) (2009) 803-810. DOI: 10.1016/j.ijrmms.2008.09.002

11. Ferentinou M., Fakir M., "An ANN Approach for the Prediction of Uniaxial Compressive Strength, of Some Sedimentary and Igneous Rocks in Eastern KwaZulu-Natal", Procedia Engineering, Vol. 191 (2017) 11117-1125.

12. Ceryan N., "Application of support vector machines and relevance vector machines in predicting uniaxial compressive strength of volcanic rocks", Journal of African Earth Sciences, Vol. 100 (2014) 634–644. DOI:10.1016/j.jafrearsci.2014.08.006

13. Cevik A., Sezer E. A., Cabalar A. F., Gokceoglu C., " Modeling of the unconfined compressive strength of some clay-bearing rocks using neural network", Applied Soft Computing, Vol. 11(2) (2011) 2587–2594. DOI: 10.1016/j.asoc.2010.10.008

14. Armaghani DJ, Safari V, Fahimifar A, Monjezi M, Mohammadi M.A., "Uniaxial compressive strength prediction through a new technique based on gene expression programming", Neural Computing and Applications 30(11) (2018) 3523–3352.

15. Mohamad E.T., Armaghani D.J., Momeni E., Yazdavar A.H., Ebrahimi M., "Rock strength estimation: a PSO-based BP approach". Neural Computing and Applications 30(5) (2018):1635–1646.

16. Sonmez H., Gokceoglu C., Nefeslioglu H. A., Kayabasi A., "Estimation of rock modulus: for intact rocks with an artificial neural network and for rock masses with a new empirical equation", International Journal Rock Mechanic and Mining Science, Vol. 43(2) (2006) 224–235. DOI: 10.1016/j.ijrmms.2005.06.007

17. Yagiz S., Sezer E. A., Gokceoglu C., "Artificial neural networks and nonlinear regression techniques to assess the influence of slake durability cycles on the prediction of uniaxial ompressive strength and modulus of elasticity for carbonate rocks", International Journal for

Numerical and Analytical Methods in Geomechanics, Vol. 36(14) (2012) 1636–1650. DOI: 10.1002/nag.1066

18. Zorlu K., Gokceoglu C., Ocakoglu F., Nefeslioglu H. A., Acikalin S. "Prediction of uniaxial compressive strength of sandstones using petrography-based models", Engineering Geology, Vol. 96(3) (2008) 141–158. DOI:10.1016/j.enggeo.2007.10.009

19. Ceryan N., Okkan U., Kesimal A., "Prediction of unconfined compressive strength of carbonate rocks using artificial neural networks", Environmental Earth Sciences, Vol. 68(3) (2013) 807-819. DOI:10.1007/s12665-012-1783-z

20. Aboutaleb, S., Behnia, M., Bagherpour, R. Bluekian, B., " Using non-destructive tests for estimating uniaxial compressive strength and static Young's modulus of carbonate rocks via some modeling techniques", Bulletin of Engineering Geology and the Environment, Vol. 77 (2018), 1717–1728 (2018).

21. Feng X., Jimenez R., "Bayesian prediction of elastic modulus of intact rocks using their uniaxial compressive strength", Engineering Geology, Vol. 173 (2014) 32–40. DOI:10.1016/j.enggeo.2014.02.005

22. Ng I. T., Yuen K. V., Lau C. H., "Predictive model for uniaxial compressive strength for grade III granitic rocks from Macao", Engineering Geology, Vol. 199 (2015) 28–37. DOI:10.1016/j.enggeo.2015.10.008

23. Wang Y., Aladejare A. E., "Selection of site-specific regression model for characterization of uniaxial compressive strength of rock", International Journal of Rock Mechanics & Mining Sciences, Vol. 75 (2015) 73-81. DOI:10.1016/j.ijrmms.2015.01.008

24. Gokceoglu C., "A fuzzy triangular chart to predict the uniaxial compressive strength of Ankara agglomerates from their petrographic composition", Engineering Geology, Vol. 66(1) (2002) 39–51. DOI:10.1016/S0013-7952(02)000236

25. Gokceoglu C., Sonmez H., Zorlu K., "Estimating the uniaxial compressive strength of some clay-bearing rocks selected from Turkey by nonlinear multivariable regression and rule-based fuzzy models", Expert System, Vol. 26(2) (2009) 176–190. DOI:10.1111/j.1468-0394.2009.00475.x

26. Karakus M., Tutmez, B., "Fuzzy and multiple regression modelling for evaluation of intact rock strength based on point load, Schmidt hammer and sonic velocity", Rock Mechanics and Rock Engineering, Vol. 39(1) (2006) 45–57. DOI:10.1007/s00603-005-0050-y

27. Jahed Armaghani D., Amin M. F., Yagiz S., Shirani Faradonbeh R., AsnidaAbdullah R., "Prediction of the uniaxial compressive strength of sandstone using various modeling techniques", International Journal of Rock Mechanics and Mining Sciences, Vol. 85 (2016) 174-186. DOI: 10.1016/j.ijrmms.2016.03.018

28. Sharma L.K., Vishal V., Singh T.N., "Developing novel models using neural networks and fuzzy systems for the prediction of strength of rocks from key geomechanical properties", Journal of Measurement ,Vol. 102 (2017) 158–169.

29. Liang M., Tonnizam Mohamad E., ShiraniFaradonbeh R., Jahed Armaghani D., Ghoraba S. "Rock strength assessment based on regression tree technique", Engineering with Computers, Vol. 32(2) (2016) 343–354. DOI: 10.1007/s00366-015-0429-7

30. Tiryaki B., "Predicting intact rock strength for mechanical excavation using multivariate statistics, artificial neural networks, and regression trees", Engineering Geology, Vol. 99(1) (2008) 51–60. DOI:10.1016/j.enggeo.2008.02.003

31. Ren Q., Wang G., Li M., Han S., Prediction of rock compressive strength using machine learning algorithms based on spectrum analysis of geological hammer. Geotechnical and Geological Engineering Vol. 37 (2019) 475–489.

32. Canakci H., Baykasoglu A., Gullu H., "Prediction of compressive and tensile strength of Gaziantep basalts via neural networks and gene expression programming", Neural Computing and Applications, Vol. 18 (2009) 1031–1041. DOI:10.1007/s00521-008-0208-0

33. Momeni E., Jahed Armaghani D., Hajihassani M., Amin M. F. "Prediction of uniaxial compressive strength of rock samples using hybrid particle swarm optimization-based artificial neural networks", Journal of Measurement, Vol. 60 (2015) 50-63. DOI:10.1016/j.measurement.2014.09.075

34. Teymen A., Cemal Mengüç E. "Comparative evaluation of different statistical tools for the prediction of uniaxial compressive strength of rocks", Vol. 30(6) (2020) 785-797

35. Tonnizam Mohamad E., Armaghani D. J., Momeni e., Alavi Nezhad S. K. "Prediction of the unconfined compressive strength of soft rocks: a PSO-based ANN approach", Bull Eng Geol Environ, VoL. 74(3) (2015) 745–757. DOI:10.1007/s10064-014-0638-0

36. Amemiya T. "Advanced Econometrics. s.l. : Harvard University Press, (1985).

37. Kramer R. "Chemometric Techniques for Quantitative Analysis." New York, (1998).

38. Liu R. X. Kuang J., Gong Q., Hou X. L., "Principal component regression analysis with SPSS", Computer Methods and Programs in Biomedicine, Vol. 71(2) (2003) 141-147. DOI: 10.1016/S0169-2607(02)00058-5

39. Vapnik V. "Nature of Statistical Learning Theory". New York, (1995).

40. Abedi M., Norouzi G. H., Bahroudi A., "Support vector machine for multi-classification of mineral prospectivity areas", Computers & Geosciences, Vol. 46 (2012) 272–283. DOI: 10.1016/j.cageo.2011.12.014

41. Zuo R. & Carranza E. J. M., "Support vector machine: A tool for mapping mineral prospectivity", Computers & Geosciences, Vol. 37(12) (2011) 1967–1975. DOI:10.1016/j.cageo.2010.09.014

42. Basak D., Pal S., ChandraPatranabis D., "Support Vector Regression", Neural Information Processing – Letters and Reviews, (2007) 11.

43. Smola A. J., Schölkopf B., "A tutoria on support vector regression", Statistics and Computing, Vol. 14, No. 3 (2004) 199–222

44. Mozumder R. A., Roy B., Laskar A. I., "Support Vector Regression Approach to Predict the Strength of FRP Confined Concrete", Arabian Journal for Science and Engineering, Vol. 42(3) (2017) 1129-1146. DOI: 10.1007/s13369-016-2340-y

45. Hatheway W. The complete ISRM suggested methods for rock characterization testing and monitoring, NEW YORK, (2009).

46. Starzec P. "Dynamic elastic properties of crystalline rocks from south-west Sweden", International Journal Rock Mechanic and Mining Science, Vol. 36(2) (1999) 265–272. DOI: 10.1016/S01489062 (99)00011-X

47. Bai S. B., Wang J., Pozdnoukhov A., Kanevski M., "Validation of logistic regression models for landslide susceptibility maps", Los Angeles, World congress on computer science and information engineering, (2009) 355–358.

48. Looney C. G. "Advances in feed forward neural networks: demystifying knowledge acquiring black boxes", IEEE Trans Knowl. Data Eng, Vol.8(2) (1996), 211–226. DOI: 10.1109/69.494162

49. Sonmez H., Gokceoglu C., Nefeslioglu H. A., Kayabasi A., "Estimation of rock modulus: for intact rocks with an artificial neural network and for rock masses with a new empirical equation" , International Journal Rock Mechanic and Mining Science, Vol. 43(2) (2006) 224–235. DOI: 10.1016/j.ijrmms.2005.06.007

50. Mokhtari A. R. "Hydrothermal alteration mapping through multivariate logistic regression analysis of lithogeochemicaldata", Journal of Geochemical Exploration, Vol. 145 (2014) 207–212. DOI: 10.1016/j.gexplo.2014.06.008

51. Jiang M., Jiang S., Zhu L., Wang Y., Huang W., & Zhang H., "Study on Parameter Optimization for Support Vector Regression in Solving the Inverse ECG Problem", Computational and Mathematical Methods in Medicine, (2013).

52. Novitasari D., Cholissodin I., Mahmudy W. F., "Optimizing SVR using Local Best PSO for Software Effort Estimation", Journal of Information Technology and Computer Science, Vol. 1(1) (2016) 28 – 37. DOI: 10.25126/jitecs.2016117